

LETTER

Mechanism for the dissolution of olivine series minerals in acidic solutions

YUN LIU,[†] AMANDA A. OLSEN, AND J. DONALD RIMSTIDT^{*}

Department of Geosciences, Virginia Tech, 4044 Derring Hall, Blacksburg, Virginia 24061, U.S.A.

ABSTRACT

The complexity of silicate minerals makes prediction of their dissolution rates a challenging problem. A combination of large cluster ab-initio quantum mechanical models and chemical probe dissolution experiments are used to understand the dissolution process for olivine-group minerals. Rapid release of M^{2+} cations by precursor reactions involving H^+ attack at μ_3 -O surface sites produces a silica-enriched surface. Slower rates of silica release via a ligand exchange reaction involving a proton in the activated complex controls the overall rate of olivine dissolution. Our results provide a physical explanation for the correlation among olivine dissolution rates and water exchange rates for the corresponding aqueous cation.

Keywords: Forsterite, dissolution rate, quantum mechanical model, ligand promoted, proton promoted

INTRODUCTION

We live in a silicate world. The Earth's crust contains 62.7 mol% oxygen and 22.0 mol% silicon so that silicate minerals dominate its mineralogy by comprising 88 wt% of the crust. Because of their abundance, reactions among silicate minerals and aqueous solutions effectively buffer the long-term composition of surface waters, soils, sediments, and the atmosphere. Many of these reactions are relatively slow so the geochemical impact of each reaction is strongly dependent upon its reaction kinetics. Because of the structural and chemical complexity of silicate minerals, the details of their reaction mechanisms remain elusive. Knowledge of reaction mechanisms is essential because they constrain the forms of the rate laws that describe the overall course of the reactions. We have developed a comprehensive strategy for establishing the reaction mechanism for silicate minerals reacting with aqueous solutions by combining experiments that use chemical probes with large cluster ab-initio quantum mechanical models. We believe that this strategy is the most effective way to understand the kinetics of silicate mineral reactions. Our approach is demonstrated by considering the reaction among forsterite (Mg_2SiO_4) and acidic solutions.

Several experimental strategies have been applied to identifying the reaction mechanisms for mineral dissolution. For example, instead of studying complicated silicate minerals, simpler Keggin molecules can be used as model systems to study the reactive sites and oxygen exchange rates on oxide surfaces and many insightful results have been obtained (Casey and Swaddle 2003; Phillips et al. 2000; Furrer et al. 1999; Rustad et al. 2004). Another obvious and widely used strategy is to study the dissolution behavior of the relatively simple olivine-group minerals as model systems. These studies have identified four important phenomena that a rate model must explain. First, olivine minerals dissolve more rapidly with declining pH (Fig.

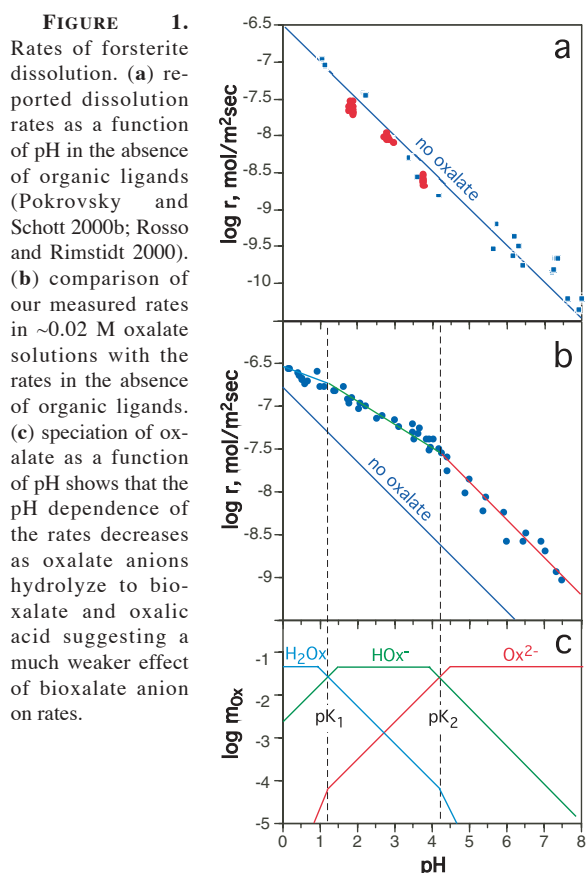
1a) (Pokrovsky and Schott 2000b; Rosso and Rimstidt 2000). This has been termed proton-promoted dissolution. Second, olivine minerals dissolve more rapidly in the presence of organic ligands (Fig. 1b) (Wogelius and Walther 1991, 1992). This has been termed ligand-promoted dissolution. Third, in acidic solutions olivine minerals release cations more rapidly than silica during the initial stages of dissolution but dissolve congruently thereafter (Pokrovsky and Schott 2000a; Rosso and Rimstidt 2000). XPS observations of acid reacted grains confirm that this initial incongruent dissolution produces a silica-enriched surface (Pokrovsky and Schott 2000a; Seyama et al. 1996). Fourth, the dissolution rate of olivine series minerals correlates with the rates of water exchange with the corresponding $M^{2+}(aq)$ cations (Casey and Westrich 1992).

Another approach to establish reaction mechanisms for silicate minerals uses ab-initio quantum chemistry calculations to model the interactions among aqueous species and small clusters of silicate atoms (Casey et al. 1990; Gibbs 1982; Lasaga and Gibbs 1990; Xiao and Lasaga 1994a, 1994b; Pelmentschikov et al. 2000a, 2000b; Felipe et al. 2004). Recently, larger and more realistic clusters of mineral structures have been used for this purpose (Rustad et al. 2004; Criscenti et al. 2005). Larger cluster simulations of mineral surfaces provide insight into how the interactions among the various surface sites affect their reactivity.

Our research, which focuses on the dissolution behavior of forsterite (Mg olivine), first investigated the precursor reactions that are responsible for the rapid release of cations leading to a silica-enriched surface. Our quantum mechanical simulations of the interaction of (001), (111), and $(2, \bar{2}, \bar{3})$ crystal planes with acidic aqueous solutions used large cluster models like that in Figure 2. More than 200 atoms are in each model. The bottom layer of atoms in each model was anchored at crystallographic locations. When the surface atoms interacted with water molecules and protons, the unconstrained surface layers expanded toward the bulk solution. The bond lengths among the outermost atoms were strongly affected by the degree of protonation of the μ_3 -O sites but not μ_2 -O sites [see one magnified μ_3 -O site on the

* E-mail: jdr02@vt.edu

[†] Present address: Geochemistry Institute, Chinese Academy of Sciences, 46 Guanshui Road, Guiyang, 550002, P.R. China.



(001) surface in Fig. 2]. If these μ_3 -O sites are not protonated, the three adjacent bonds are quite short (even shorter than in the crystal) and the μ_3 -O atoms sink into the surface. This results in strong bonding among the adjacent atoms and the μ_3 -O sites and makes the surface stable. Upon protonation, the three bonds around the μ_3 -O sites lengthen dramatically (Fig. 2) making them more labile and this leads to bond breaking as shown in Figure 3. The μ_3 -OH site is a strong Brønsted acid, which is not easily protonated unless the pH is low. Similar cluster models of Keggin molecules showed that oxygen exchange rates of μ_2 -O sites are much faster than aluminum release rates and are independent of the pH (Phillips et al. 2000, 2003; Furrer et al. 1999; Casey et al. 2000; Casey and Phillips 2001; Lee et al. 2002). The protonation of μ_2 -O sites leads to rapid bond breaking compared to the structure breaking process that releases silica. Thus, our model results are similar to those that show that the protonation of μ_4 -O sites in Al Keggin molecules leads to structure breaking (Casey et al. 2000).

Consistent with reported results (Awad et al. 2000), the stability of the μ_3 -O sites depends upon the crystallographic orientation of the exposed surface. For example the μ_3 -O site is relatively stable on the (2, $\bar{2}$, $\bar{3}$) surface because of its highly symmetric setting. However, protonation of the μ_3 -O site on the edges of the (111) surface model caused the M-O bonds to break. Bond breaking around protonated μ_3 -O sites in smaller cluster models without fixed atoms was common, suggesting that kink or edge sites with geometries that are only weakly constrained by the bulk structure are subject to large bond length distortions making them especially unstable. In all cases the bonds break

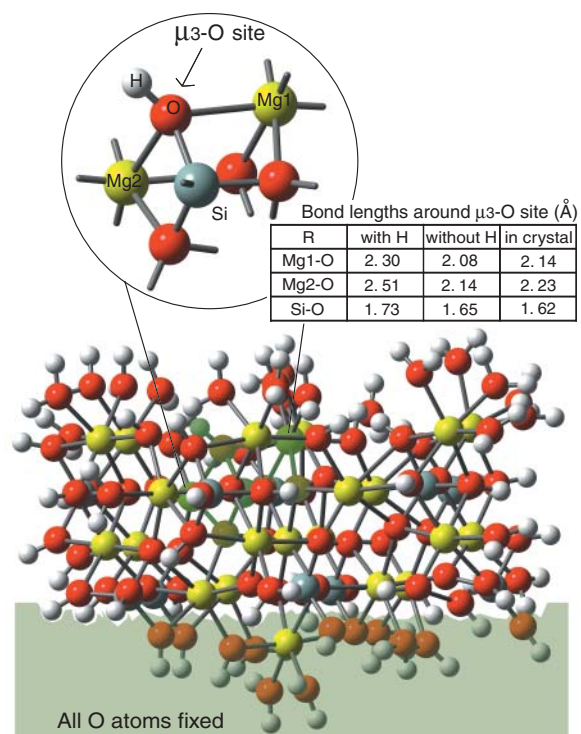
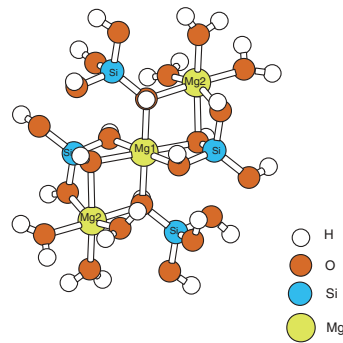


FIGURE 2. Model of hydrated and protonated (001) plane in forsterite showing how the attachment of a proton to a μ_3 -O site significantly lengthens and weakens the bonds holding Mg^{2+} . The Mg-O bonds disappeared in similar models for other crystallographic planes. In this model the O atoms in the shaded region were all fixed to their crystallographic positions and the atoms above relaxed to the minimum energy configuration.

between Mg and O atoms leaving the O atom with its affixed proton attached to the adjacent silica group. As the Mg-O bonds break, water molecules coordinate the Mg^{2+} ion until it eventually dissociates from the surface as $Mg^{2+}(H_2O)_6$. The departing Mg^{2+} ion carries away the positive charge that had been deposited on the surface by the protonation steps. The SiO_4 units remain tightly linked to the bulk structure after the departure of Mg^{2+} from the surface layer.

The silica enriched surface predicted by our ab initio quantum mechanical model appears to be relatively stable suggesting that the rate determining step for the overall dissolution process is the release of silica from the surface. Many previous experiments showed that the overall dissolution rate of forsterite depends upon pH, suggesting that a proton participates in the activated complex for the rate-determining step. Our experiments (Fig. 1b) over the pH range of 0 to 8 show a similar pH dependence for the rate of olivine dissolution in the presence of ~ 0.02 M total oxalate as well as when no oxalate is present. This means that a proton must also be present in the activated complex when an organic ligand participates in the dissolution process. For $pH > 4.19$ (pK_2), where oxalate ion is the predominant form of oxalic acid (Fig. 1c), the pH dependence of olivine dissolution rates is the same as for solutions without added organic ligands. However, when $pH < 4.19$ (pK_2), the rates depend upon a balance between the degree of surface protonation and the ligand protonation so

FIGURE 3. Illustration a of bond breaking at kink edges or in small clusters caused by the protonation of the μ_3 -O site. (a) Optimization of the input cluster with protons attached to μ_3 -O sites leads to (b), the structure with broken bonds.



that as the concentration of unprotonated oxalate ion declines at lower pH, its ability to enhance the dissolution rate also declines.

These results, and the observation that attachment of protons to connecting O atoms leads to breaking of bonds among Mg^{2+} and adjacent O atoms, lead us to propose the structure shown in Figure 4 as the activated complex for the rate determining silica release step for olivine dissolution. In this figure we show water as a ligand that over-coordinates a Mg site leading to the breaking of the Mg-OH bond that tethers a silica moiety to the surface. Oxalate and similar organic ligands enhance olivine dissolution rates because they are more effective in over-coordinating the M site to produce the ligand exchange reaction posited here. The release of silica leaves a surface region with a stoichiometric amount of Mg that is subsequently released by the rapid precursor reactions described above.

Figure 4 suggests that silica can be released when either H_2O or an oxalate ion attacks and over-coordinates an Mg site that is connected to tethered silica. Because these ligand exchange reactions occur in parallel, the form of a rate law for olivine dissolving in an aqueous solution containing an organic ligand (L) that can attack the Mg site should be of the form

$$r = A(k_1 a_H^n a_{H_2O}^m + k_2 a_L^{n_2} a_L^{m_2})$$

where r is the observed release rate, A is the surface area of the mineral, k_1 and k_2 are rate constants for two independent reactions, a is the activity of the subscripted species, and n and m represent reaction orders for the subscripted species. The rate constant, k_2 , for the reaction involving the ligand is much larger than k_1 for the reaction involving water molecules because of the higher charge on the ligand compared to the water dipole.

This model of the activated complex for the rate determining step is further substantiated by another quantum mechanical model that shows that dissolution rates of olivine series minerals are proportional to the length of the bond to the M site (Fig. 5), where the O is a μ_2 -OH site connecting the silica to the M site. Bond strength (s), as defined by Brown and Shannon (1973) [$s = (R/R_0)^{-N}$] is closely related to bond length. Our simple cluster

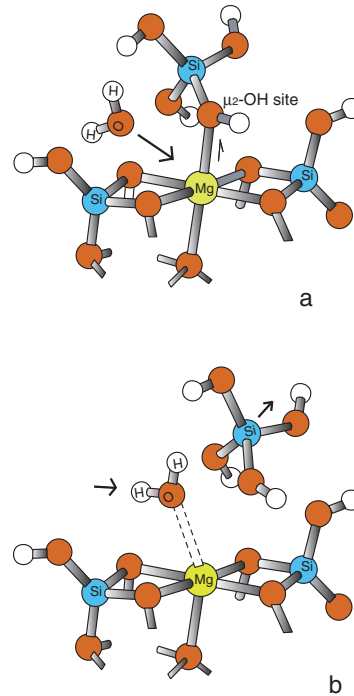


FIGURE 4. Schematic illustration of the proposed rate-determining step, which occurs after the fast precursor reactions release Mg from the surface (on a silica rich surface). (a) The activated complex consists of a silicic acid group attached to a Mg site. (b) When a ligand (in this case a water molecule) attaches to and over coordinates the Mg atom it causes the bond between the Mg and μ_2 -OH site to break releasing silicic acid to solution. The rate of silica release is proportional to the strength of interaction of the ligand with the Mg atom.

model shown in Figure 5 has a structure like the one shown in Figure 4 but the Mg atom is not embedded in a mineral surface. Replacing M^{2+} with different cations and optimizing the structure at the B3LYP/6-311+G** level predicts the M^{2+} -O (μ_2 -OH site) bond lengths shown by the red squares in Figure 5. The graph of these bond length shows a good correlation with experimental olivine mineral dissolution rates. As the M-O bond length in the cluster increases, the attacking ligand can approach the M site more readily so the rate of the ligand exchange step becomes faster. The dissolution rates of olivine series minerals can be accurately predicted by using bond lengths calculated from this model. Figure 5 shows dissolution rates predicted by our model for some olivine minerals (Brown 1982) for which no rate mea-

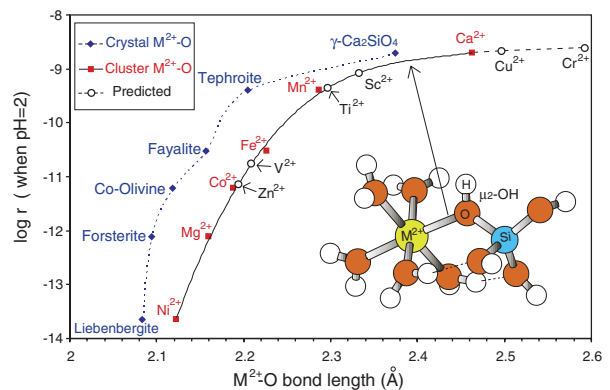


FIGURE 5. Correlation between modeled length of the bond, which links the M^{2+} cation to the μ_2 -OH site in a series of olivine minerals, and the dissolution rate for the corresponding M_2SiO_4 olivine. The M^{2+} -O bond lengths for the crystal are based on the smaller M1 site average data; the M^{2+} -O bond lengths are optimized results based on the cluster model shown.

surements exist. A less accurate correlation is formed among crystal M^{2+} -O bond lengths and the dissolution rate (as shown in dash line with diamonds). Because many silicate minerals have similar pH-dependent dissolution patterns, our finding can help to understand their dissolution mechanisms.

The correlation among mineral dissolution rates and ligand exchange rates is well documented (Casey and Westrich 1992). We hope that our experiments and models have provided a better insight into the reason for this correlation.

METHODS

Olivine ($fo_{0.92}$) from Aimcor Mine, Green Mountain, North Carolina, U.S.A. was used for the experiments. Prior to rate determinations, the 250–350 μm grains were pre-treated by sonicating in 1 M HNO_3 10 times each for 1 min, as well as soaking in 6 M HNO_3 overnight to create a silica-enriched surface. Eighty-five 2-h dissolution experiments were run at 25 °C in 250 mL Erlenmeyer flasks immersed in a shaker bath. Each flask contained approximately 5 g of forsterite and 100 mL of ~0.02 M oxalate solution adjusted to a pH among 0 and 8. Approximately 6 mL of solution was collected at 20 min intervals. Solutions were analyzed for Mg using Atomic Absorbance spectrophotometry. Silica concentrations were determined using the molybdate blue colorimetric method. Rates were calculated using the initial rate method.

All geometry optimization calculations were performed using the B3LYP DFT (density functional theory) method with Becke's three-parameter hybrid functional using the LYP correlation functional and GAUSSIAN 03 (Becke 1993; Lee et al. 1988; Frisch et al. 2004). The basis set was the standard polarized split-valence 6-31G*. B3LYP/6-311+G** level was used for some small clusters with H-bonding for transition metals studied here. The Wachters-Hey basis set (Wachters 1970; Hay and Dunning 1977) with different scaling factors and diffuse functions were used for the first row transition elements in the Gaussian code for 6-311+G** basis set. Cluster models for the crystal planes (001), (111) and (2,2,3) were built using the X-ray coordinates as starting points. At least $5 \times 6 \times 6$ layers of atoms were truncated to make a fragment for building a cluster model. To further constrain the bulk structure, the positions of bottom layer atoms were fixed to their X-ray coordinates. Several atoms at the lower sides were also fixed to represent the constraints from the side directions. Then OH and H_2O groups were added to the under-bonded sites on the surface of the entire fragment to create fully hydrated surfaces. H_2O was added to Mg sites and OH was added to Si sites to represent a protonated surface expected at low pH. All the μ_2 -O sites were protonated to form μ_2 -OH. This produced a positively charged surface like that reported for acid titrations of olivines. In addition to this kind of surface, a similar cluster model with all μ_3 -O sites at top surface protonated was also constructed by adding several more H^+ . Then both the μ_3 -O surface and the μ_2 -OH surface were optimized on a SGI ALTIX 3700 supercomputer and several DELL dual CPU workstations. Many clusters used here have large sizes with more than 4000 primitive Gaussian functions (see supporting material). The optimized structures (e.g., relaxed bond length) were then carefully analyzed to identify possible bond-breaking pathways.

ACKNOWLEDGMENTS

This work was supported by the U.S. Department of Energy Basic Energy Sciences grant DE-FG02-03ER14751. We thank Jerry Gibbs for his input to this project.

REFERENCES CITED

- Awad, A., Koster van Groos, A.F., and Guggenheim, S. (2000) Forsteritic olivine: Effects of crystallographic direction on dissolution kinetics. *Geochimica et Cosmochimica Acta*, 64, 1765–1772.
- Becke, A.D. (1993) A new mixing of Hartree-Fock and local density functional theories. *Journal of Chemical Physics*, 98, 1372–1377.
- Brown, G.E. (1982) Olivines and silicate spinels. In P.H. Ribbe, Ed., *Orthosilicates*, 5, p. 275–381. *Reviews in Mineralogy*, Mineralogical Society of America, Chantilly, Virginia.
- Brown, I.D. and Shannon, R.D. (1973) Empirical bond-strength-bond-length curves for oxides. *Acta Crystallographica A*, 29, 266–280.
- Casey, W.H. and Phillips, B.L. (2001) The kinetics of oxygen exchange between sites in the $\text{GaO}_4\text{Al}_{12}(\text{OH})_{24}(\text{H}_2\text{O})_{12}^{7-}(\text{aq})$ molecule and aqueous solution. *Geochimica et Cosmochimica Acta*, 65, 705–714.
- Casey, W.H. and Swaddle, T.W. (2003) Why small?—the use of small inorganic clusters to understand mineral surface and dissolution reactions in geochemistry. *Reviews in Geophysics*, 41, 4.1–4.20.
- Casey, W.H. and Westrich, H. (1992) Control of dissolution rates of orthosilicate minerals by divalent metal-oxygen bonds. *Nature*, 355, 157–159.
- Casey, W.H., Lasaga, A.C., and Gibbs, G.V. (1990) Mechanisms of silica dissolution as inferred from the kinetic isotope effect. *Geochimica et Cosmochimica Acta*, 54, 3369–3378.
- Casey, W.H., Phillips, B.L., Karlsson, M., Nordin, S., Nordin, J.P., Sullivan, D.J., and Neugebauer-Crawford, S. (2000) Rates and mechanism of oxygen exchanges between sites in the $\text{AlO}_4\text{Al}_{12}(\text{OH})_{24}(\text{H}_2\text{O})_{12}^{7-}(\text{aq})$ complex and water: Implications for mineral surface chemistry. *Geochimica et Cosmochimica Acta*, 64, 2951–2964.
- Criscenti, L.J., Brantley, S.L., Mueller, K.T., Tsomaia, N., and Kubicki, J.D. (2005) Theoretical and ^{27}Al CP/MAS NMR investigation of aluminum coordination changes during aluminosilicate dissolution. *Geochimica et Cosmochimica Acta*, 69, 2205–2220.
- Felipe, M.A., Kubicki, J.D., and Rye, D.M. (2004) Oxygen isotope exchange kinetics between H_2O and H_4SiO_4 from ab initio calculations. *Geochimica et Cosmochimica Acta*, 68, 949–958.
- Frisch, M.J., Trucks, G.W., Schlegel, H.B., Scuseria, G.E., Robb, M.A., Cheeseman, J.R., Montgomery, J.A., Jr., Vreven, T., Kudin, K.N., Burant, J.C., and others. (2004) Gaussian 03, Revision B.05. Gaussian, Inc., Wallingford, Connecticut.
- Furrer, G., Gfeller, M., and Wehrli, B. (1999) On the chemistry of the Keggin Al-13 polymer-kinetics of proton-promoted dissolution. *Geochimica et Cosmochimica Acta*, 63, 3069–3076.
- Gibbs, G.V. (1982) Molecules as models for bonding in silicates. *American Mineralogist*, 67, 421–450.
- Hay, P.J. and Dunning, T.H. (1977) Geometries and energies of excited states of O^{3-} from ab initio potential-energy surfaces. *Journal of Chemical Physics*, 67, 2290–2303.
- Lasaga, A.C. and Gibbs, G.V. (1990) Ab initio quantum-mechanical calculations of water-rock interactions—adsorption and hydrolysis reactions. *American Journal of Science*, 290, 263–295.
- Lee, A.P., Phillips, B.L., and Casey, W.H. (2002) The kinetics of oxygen exchange between $\text{GeO}_4\text{Al}_{12}(\text{OH})_{24}(\text{OH})_{12}^{7-}(\text{aq})$ molecule and aqueous solution. *Geochimica et Cosmochimica Acta*, 66, 577–587.
- Lee, C., Yang, W., and Parr, R.G. (1988) Development of the Colle-Salvetti correlation-energy formula into a functional of the electron density. *Physical Reviews B*, 37, 785–789.
- Pelmenschikov, A., Leszczynski, J., and Pettersson, L.G.M. (2000a) Mechanism of dissolution of neutral silica surfaces: including effect of self-healing. *Journal of Physical Chemistry A*, 105, 9528–9532.
- Pelmenschikov, A., Strandh, H., Pettersson, L.G.M., and Leszczynski, J. (2000b) Lattice resistance to hydrolysis of Si-O-Si bonds of silicate minerals: ab initio calculations of a single water attack onto the (001) and (111) beta-cristobalite surfaces. *Journal of Physical Chemistry B*, 104, 5779–5783.
- Phillips, B.L., Casey, W.H., and Karlsson, M. (2000) Bonding and reactivity at oxide mineral surfaces from model aqueous complexes. *Nature*, 404, 379–382.
- Phillips, B.L., Lee, A.P., and Casey, W.H. (2003) Rates of oxygen exchange between the $\text{Al}_2\text{O}_3\text{Al}_{24}(\text{OH})_{36}(\text{H}_2\text{O})_{24}^{18-}(\text{aq})$ (Al_{30}) molecule and aqueous solutions. *Geochimica et Cosmochimica Acta*, 67, 2725–2733.
- Pokrovsky, O.S. and Schott, J. (2000a) Forsterite surface composition in aqueous solutions: A combined potentiometric, electrokinetic, and spectroscopic approach. *Geochimica et Cosmochimica Acta*, 64, 3299–3312.
- — — (2000b) Kinetics and mechanism of forsterite dissolution at 25 °C and pH from 1 to 12. *Geochimica et Cosmochimica Acta*, 64, 3313–3325.
- Rosso, J.J. and Rimstidt, J.D. (2000) A high resolution study of forsterite dissolution rates. *Geochimica et Cosmochimica Acta*, 64, 797–811.
- Rustad, J.R., Loring, J.S., and Casey, W.H. (2004) Oxygen-exchange pathways in aluminum polyoxocations. *Geochimica et Cosmochimica Acta*, 68, 3011–3017.
- Seyama, H., Soma, M., and Tanaka, A. (1996) Surface characterization of acid-leached olivines by X-ray photoelectron spectroscopy. *Chemical Geology*, 129, 209–216.
- Wachters, A.J.H. (1970) Gaussian basis set for molecular wave functions containing third-row atoms. *Journal of Chemical Physics*, 52, 1033–1036.
- Wogelius, R. and Walther, J. (1991) Olivine dissolution at 25 °C: Effects of pH, CO_2 , and organic acids. *Geochimica et Cosmochimica Acta*, 55, 943–954.
- — — (1992) Olivine dissolution kinetics at near-surface conditions. *Chemical Geology*, 97, 101–112.
- Xiao, Y.T. and Lasaga, A.C. (1994a) Ab initio quantum mechanical studies of the kinetics and mechanisms of silicate dissolution— $\text{H}^+(\text{H}_3\text{O}^+)$ catalysis. *Geochimica et Cosmochimica Acta*, 58, 5379–5400.
- — — (1994b) Ab initio quantum mechanical studies of the kinetics and mechanisms of quartz dissolution: OH^- catalysis. *Geochimica et Cosmochimica Acta*, 60, 2283–2295.

¹ Deposit item AM-06-011, supporting materials. Deposit items are available two ways: For a paper copy contact the Business Office of the Mineralogical Society of America (see inside front cover of recent issue) for price information. For an electronic copy visit the MSA web site at <http://www.minsocam.org>, go to the American Mineralogist Contents, find the table of contents for the specific volume/issue wanted, and then click on the deposit link there.